JACS
JOURNAL OF THE AMERICAN CHEMICAL SOCIETY
Article
pubs.acs.org/JACS

# Photon Upconversion in Supramolecular Gel Matrixes: Spontaneous Accumulation of Light-Harvesting Donor–Acceptor Arrays in Nanofibers and Acquired Air Stability

Pengfei Duan,[†] Nobuhiro Yanai,*[,†,‡] Hisanori Nagatomi,[†] and Nobuo Kimizuka*[,†]

[†]Department of Chemistry and Biochemistry, Graduate School of Engineering, Center for Molecular Systems (CMS), Kyushu University, 744 Moto-oka, Nishi-ku, Fukuoka 819-0395, Japan

[‡]PRESTO, JST, Honcho 4-1-8, Kawaguchi, Saitama 332-0012, Japan

Supporting Information

**ABSTRACT:** Efficient triplet–triplet annihilation (TTA)-based photon upconversion (UC) is achieved in supramolecular organogel matrixes. Intense UC emission was observed from donor (sensitizer)–acceptor (emitter) pairs in organogels even under air-saturated condition, which solved a major problem: deactivation of excited triplet states and TTA-UC by molecular oxygen. These unique TTA-UC molecular systems were formed by spontaneous accumulation of donor and acceptor molecules in the gel nanofibers which are stabilized by developed hydrogen bond networks. These molecules preorganized in nanofibers showed efficient transfer and migration of triplet energy, as revealed by a series of spectroscopic, microscopic, and rheological characterizations. Surprisingly, the donor and acceptor molecules incorporated in nanofibers are significantly protected from the quenching action of dissolved molecular oxygen, indicating very low solubility of oxygen to nanofibers. In addition, efficient TTA-UC is achieved even under excitation power lower than the solar irradiance. These observations clearly unveil the adaptive feature of host gel nanofiber networks that allows efficient and cooperative inclusion of donor–acceptor molecules while maintaining their structural integrity. As evidence, thermally induced reversible assembly/disassembly of supramolecular gel networks lead to reversible modulation of the UC emission intensity. Moreover, the air-stable TTA-UC in supramolecular gel nanofibers was generally observed for a wide combination of donor–acceptor pairs which enabled near IR-to-yellow, red-to-cyan, green-to-blue, and blue-to-UV wavelength conversions. These findings provide a new perspective of air-stable TTA-UC molecular systems; spontaneous and adaptive accumulation of donor and acceptor molecules in oxygen-blocking, self-assembled nanomatrixes. The oxygen-barrier property of L-glutamate-derived organogel nanofibers has been unveiled for the first time, which could find many applications in stabilizing air-sensitive species in aerated systems.

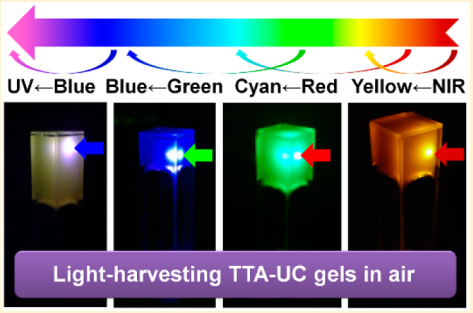


## INTRODUCTION

In biological photon harvesting systems such as those found in thylakoid membranes or purple bacteria, supercomplexes of photosystem I and II and a host of membrane-bound peripheral antenna complexes are self-assembled in biomembranes.[1] The dense accumulation and controlled alignment of these functional elements in two-dimensional lipid nanomatrixes allow efficient excitation energy transfer and migration toward the reaction center, which is followed by subsequent photosynthetic chemical reactions.[1] Inspired by the photosynthetic light conversion systems, self-assembly of photofunctional molecules in ordered nanoarchitectures has been one of the up-front areas in chemistry.[2] Although chemistry offers the advantages of a variety of molecular designs for unit molecules and their regular self-assembly, biological photon harvesting systems in terms of their sophisticated architectures and performances are still far beyond the synthetic model systems. In this light, it is essential to embody the archetypal essence of the role of photosynthetic biomembranes: adaptive accommodation of supercomplexes in high density and regulation of the lateral diffusion of excitation energy and molecular electron shuttles in confined space, which forms the basis of efficient biological photosynthetic systems.

With these in mind, we conceived an idea to integrate self-assembling nanomatrixes with photon upconversion (UC) which is based on the triplet–triplet annihilation (TTA) phenomena. TTA-based UC has attracted much attention as a promising wavelength up-shifting technology which can utilize noncoherent light sources. The characteristics of TTA-UC including the low-power excitation and high quantum yield are beneficial for practical applications, ranging from sunlight-powered renewable energy production including photovoltaics and photocatalysis to bioimaging and phototherapy.[3] This TTA-UC process occurs in association with multistep photochemical events (Figure S1, Supporting Information (SI)).

**Received:** October 28, 2014
**Published:** January 19, 2015





DOI: 10.1021/ja511061h
J. Am. Chem. Soc. 2015, 137, 1887–1894

First, a triplet excited state of donor (sensitizer) is formed by intersystem crossing from the photoexcited singlet state, and acceptor (emitter) excited triplets are populated by triplet−triplet energy transfer (TTET) from the donor triplets. When two acceptor molecules in the triplet state diffuse and come into collision during their lifetime, a higher singlet energy level is formed by TTA, which consequently produces delayed upconverted fluorescence. The excitation and emission wavelength of TTA-UC can be regulated by independent selection of sensitizers and emitters. Because of the long lifetime of the triplet species, the excitation power density can be reduced to as low as a few mW $cm^{-2}$ that is on the order of sunlight intensity at a specific excitation wavelength.

To date, most efficient TTA-UC systems have been achieved in molecularly dispersed solutions because they allow fast diffusion of excited molecules. However, they suffer from overwhelming deactivation of excited triplets by dissolved oxygen which severely limits their operation to strictly deaerated conditions. The realization of efficient TTA-UC in the ambient, oxygen-rich environment should lead not only to an improvement of efficiency but also to a myriad of applications including sunlight-powered energy production. A few reports have been made for TTA-UC under aerated conditions by employing specific solid polymers or viscous liquids as matrixes to block oxygen.[4] However, such thick matrixes inevitably restrict the diffusion of excited triplet molecules, resulting in the use of high-power incident light to ensure effective concentration of excited triplet states. Therefore, it is absolutely imperative to develop new matrixes that show oxygen blocking ability while allowing efficient TTA-UC of the incorporated donor−acceptor pairs under low-power excitation.

Inspired by the structural feature of thylakoid membranes, we have chosen supramolecular gel nanofibers as matrixes to confine sensitizer and emitter molecules (Figure 1). Supramolecular organogels are produced by the self-assembly of low-molecular-weight, lipophilic molecules which give nanofibrous networks to gelatinize organic solvents.[5] They typically possess multiple hydrogen-bonding groups and/or aromatic chromophores that enhance the cohesive energy of gelator molecules, giving long-ranged crystalline-like order while maintaining the physically cross-linked nanofiber structures. As will be understood, two complementary approaches are available to integrate self-assembly with TTA-UC: covalent modification of donor/acceptor chromophores with self-assembling moieties or confinement of the chromophores in self-assembled nanomatrixes. The covalent introduction of solvophilic groups to solvophobic chromophores to give self-assembling properties is an excellent approach in terms of controlling their morphology and molecular orientation;[5] however, it usually involves an immense amount of time and synthetic efforts.[6] Here we focus on the alternative approach and show that self-assembled nanofibers serve as adaptive nanohosts in organic media,[7] which accommodate donor and acceptor molecules to provide air-stable, photon-upconversion gels via solvophobic interactions. It provides a new perspective in organogel research because it not only offers a useful and versatile methodology to develop photon-upconverting soft materials but also a surprising potential of blocking molecular oxygen.

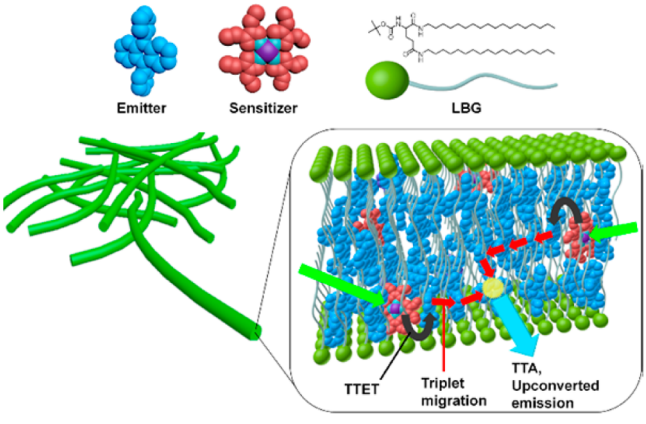


**Figure 1.** A schematic representation of the unit structure of the upconversion gel system. Donor (red) and acceptor (blue) molecules are incorporated in the LBG nanofibers as extended domains. The donor molecules are excited by long-wavelength light, followed by a sequence of triplet−triplet energy transfer (TTET) from the donor to the surrounding acceptor, triplet energy migration among the acceptor molecules, triplet−triplet annihilation (TTA), and delayed fluorescence from the upconverted singlet state of acceptor.

## EXPERIMENTAL SECTION

**Materials.** All reagents and solvents were used as received unless otherwise indicated. Palladium(II) octabutoxyphthalocyanine (PdPc-$(OBu)_8$) and platinum(II) tetraphenyltetrabenzoporphyrin (PtTPBP) were purchased from Frontier Scientific, Inc. Platinum(II) octaethylporphyrin (PtOEP), rubrene, 9,10-bis(phenyl-ethynyl)anthracene (BPEA), 9,10-diphenylanthracene (DPA), and 2,7-di-*tert*-butylpyrene (DBP) were purchased from Aldrich and TCI. $Ir(C6)_2(acac)$ (C6 = coumarin 6, acac = acetylacetone) was synthesized according to the reported methods.[8] Analytical grade dimethylformamide (DMF), carbon tetrachloride ($CCl_4$), and chloroform were purchased from Wako Pure Chemical. A gelator *N*,*N*′-bis(octadecyl)-L-boc-glutamic diamide (LBG) was synthesized according to the literature.[9] The dye-doped gels were prepared by heating a mixture of LBG, sensitizer, emitter, and solvent (DMF or $CCl_4$) at 80 °C for 2−3 min, until a clear solution was formed, and subsequent cooling to the room temperature. The gel formation was confirmed by inverse tube tests and rheology measurements. The obtained cogels were strong enough to keep their shapes more than two months without any collapse. For the preparation of the deaerated gel, first, all the solids (PtOEP, DPA, and LBG) and solvent DMF were added to a cell, where some solids remained undissolved. Second, all the gas in the dispersion was removed by repeated freeze−pump−thaw cycles. Third, the degassed dispersion was heated for 2−3 min at 80 °C by using a hot water bath until a clear solution was formed, and then the hot solution was cooled to the room temperature, providing a deaerated gel.

**Characterization.** UV−vis absorption spectra were recorded on a Jasco V-670 spectrophotometer. Luminescence spectra were measured by using a PerkinElmer LS 55 fluorescence spectrometer. Time-resolved fluorescence lifetime measurements were carried out by using a time-correlated single photon counting lifetime spectroscopy system, Hamamatsu Quantaurus-Tau C11367-02 (for fluorescence lifetime)/C11567−01 (for delayed luminescence lifetime). The quality of the fit has been judged by the fitting parameters such as $\chi^2$ (<1.2) as well as the visual inspection of the residuals. The upconversion luminescence spectra were recorded on an Otsuka Electronics MCPD-7000 instrument with the excitation source using external, adjustable semiconductor lasers. Differential scanning calorimetry (DSC) was performed in a Seiko Electronics SSC-5200 instrument. The rheology experiments were carried out using an Anton Paar MCR-302 rheometer at 25 °C. The frequency of the measurement was set as 1 Hz. Scanning electron microscopy (SEM) pictures of xerogels were taken on a Hitachi S-5000 (acceleration voltage, 10 kV). The accelerating voltage was 15 kV, and the emission was 10 mA. The xerogels were prepared by drying the gels with a Jasco SCF supercritical $CO_2$ system.[10] UC quantum yield of the cogels were


DOI: 10.1021/ja511061h
J. Am. Chem. Soc. 2015, 137, 1887−1894

measured using an absolute quantum yield measurement system using a laser excitation source and a calibrated spectrometer specially built by Hamamatsu Photonics. The quality of the integrating sphere was confirmed by using a standard anthracene solution in ethanol (45 $\mu$M, excitation at 340 nm by Xe lamp). The measured fluorescence quantum yield (0.28 ± 0.02) was close to the reported value (0.27 ± 0.03).[11] As for the laser excitation, a collimated laser beam with a diameter of ca. 1.2 mm was used. The upconversion quantum yield is given by

$$\Phi_{UC} = \frac{PN(Em)}{PN(Abs)} = \frac{\int \frac{\lambda}{\hbar c}[I_{em}^{sample}(\lambda) - I_{em}^{reference}(\lambda)]d\lambda}{\int \frac{\lambda}{\hbar c}[I_{ex}^{reference}(\lambda) - I_{ex}^{sample}(\lambda)]d\lambda}$$

where PN(Abs) is the number of photons absorbed by a sample, PN(Em) is the number of photons emitted from a sample, $\lambda$ is the wavelength, $\hbar$ is Planck's constant, $c$ is the velocity of light, $I_{em}^{sample}$ and $I_{ex}^{reference}$ are the integrated intensities of the excitation light with and without a sample respectively, and $I_{em}^{sample}$ and $I_{em}^{reference}$ are the photoluminescence intensities with and without a sample, respectively.[11b,12] Since the detector is easily saturated when a laser is used as an excitation source, the 532 nm notch filter was set before the detector to attenuate the excitation power. The sensitivity calibration of the system was performed including the notch filter. The accuracy of this sensitivity calibration was confirmed by the same quantum yields of rhodamine B with and without the filter.

## RESULTS AND DISCUSSION

As a supramolecular gelator for TTA-UC, we employed a well-known compound, *N*,*N*′-bis(octadecyl)-L-boc-glutamic diamide (LBG) (Figure 1).[9] LBG has been reported to gelatinize a wide variety of nonpolar or polar solvents, and the resultant gels show high stability.[7b,9,13] This is due to the presence of three amide groups connected to the chiral center in LBG, which gives stable hydrogen bond networks with the aid of aligned alkyl chains.[14] At the first outset, the pair of PtOEP and DPA was chosen as donor and acceptor since they have been employed as benchmark for TTA-UC in organic media. As a result, LBG formed supramolecular gels in DMF in the presence of PtOEP and DPA molecules. Homogeneous pink gel was obtained by heat-dissolving the solid powders of LBG, PtOEP, and DPA in DMF ([PtOEP] = 33 $\mu$M, [DPA] = 6.7 mM, [LBG] = 10 mg mL$^{-1}$ = 13.3 mM) and then cooling to the room temperature. The ternary organogels showed good structural stability so that a specific gel shape could be prepared by injecting the hot solutions into a mold (Figure 2a).

Figure 2c shows absorption and emission spectra for the PtOEP-containing and DPA-containing binary LBG gels, abbreviated hereafter as PtOEP/LBG and DPA/LBG gels, respectively. The spectra of PtOEP/LPG binary gel exhibited typical Soret-band at 380 nm and Q-bands at 500 and 535 nm, and a phosphorescence peak at 645 nm. The spectra of DPA/LBG gel showed a typical vibrational structure of the anthracene $L_a$ absorption, with its fluorescence observed at 435 nm. These spectra are similar to those of PtOEP or DPA in DMF solutions without LBG, indicating that the LBG molecules do not interfere with their photophysical properties. Amazingly, even in the air-saturated state, strong blue upconverted emission was observed by the naked eye from the PtOEP/DPA/LBG ternary gel upon excitation of 532 nm green laser (Figure 2b). Steady-state luminescence spectra at varied incident laser power clearly showed the upconverted emission of DPA at 435 nm (Figure 2d, excitation at 532 nm). The spectral shape of UC emission is similar to that of the inherent fluorescence of DPA directly excited at 375 nm. In Figure 2d, the intensity of PtOEP phosphorescence at 645 nm

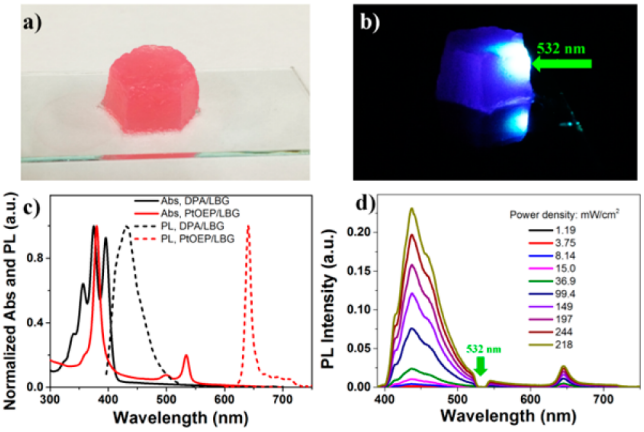


**Figure 2.** Pictures of the PtOEP/DPA/LBG ternary gel shaped in a mold under (a) white light and (b) 532 nm green laser ([PtOEP] = 33 $\mu$M, [DPA] = 6.7 mM, [LBG] = 13.3 mM). No filter was used to take the pictures. (c) Normalized absorption (solid line) and emission (dashed line) spectra of the PtOEP/LBG binary gel (red line; [PtOEP] = 33 $\mu$M, [LBG] = 13.3 mM) and the DPA/LBG binary gel (black line; [DPA] = 6.7 mM, [LBG] = 13.3 mM) in DMF. (d) Photoluminescence spectra of the PtOEP/DPA/LBG ternary gel in air-saturated DMF with different incident power density of 532 nm laser at room temperature. A notch filter at 532 nm was used to remove the scattered incident light.

is very weak, indicating that the triplet excited state of PtOEP produced by intersystem crossing showed efficient TTET to DPA. The experimental condition employed ([PtOEP] = 33 $\mu$M, [DPA] = 6.7 mM, [LBG] = 13.3 mM) was optimized based on the UC emission intensity (Table S1, SI).

This UC emission was surprisingly stable; the UC emission intensity remained almost unchanged under exposure to air for 25 days (Figure S2, SI). It is to note that such stable UC emission is not observable for the PtOEP/DPA pair in aerated DMF solution, in the absence of LBG gelator. The DMF solution showed UC emission right after the preparation; however, the UC emission almost disappeared by exposure to air for a few days, probably due to the chemical degradation of dyes by dissolved oxygen. These observations indicate that the chemical degradation by dissolved molecular oxygen is effectively prevented by the LBG gel.

**Mechanism of Air-Stable TTA-UC in Gels.** The stable TTA-UC observed in air implies the effective uptake of dye molecules in the LBG nanofibers in the course of physical gelation process, which was supported by SEM, rheology, and DSC measurements. The gel samples were dried by using supercritical $CO_2$ in order to maintain their microstructures. The SEM image of LBG xerogels showed fibrous nanostructures with an average width of 70 nm (Figure 3a). In contrast, nanofibers with enhanced width of several hundred nanometers were observed for the ternary PtOEP/DPA/LBG gel, with the maintenance of smooth surface structure (Figure 3b). The observed morphological changes of nanofibers without apparent segregation of dye molecules are interpreted by the efficient inclusion of PtOEP and DPA molecules, as further supported by the viscoelasticity measurement. The rheological property of supramolecular gels was evaluated for the linear viscoelastic regime in which storage ($G'$) and loss ($G''$) moduli become independent to the applied stress amplitude.[5a] Above a critical stress, gels partly break and begin to flow, resulting in the decrease in storage modulus. Figure 3c shows the storage


DOI: 10.1021/ja511061h
J. Am. Chem. Soc. 2015, 137, 1887−1894

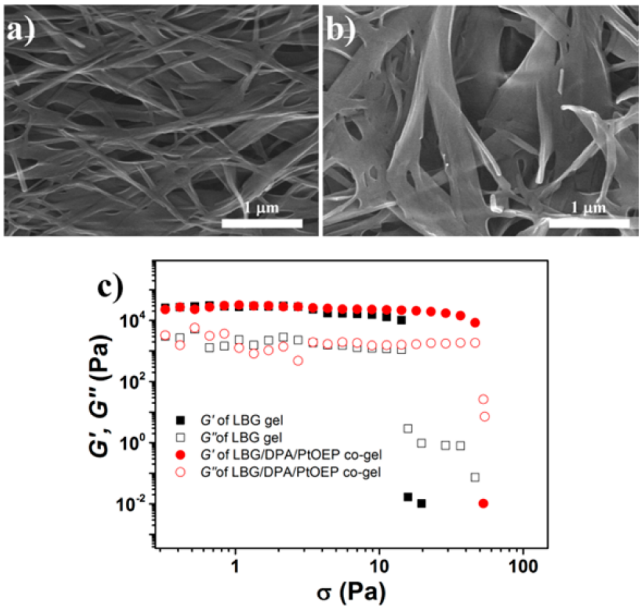


**Figure 3.** SEM images of (a) the single-component LBG gel ([LBG] = 13.3 mM) and (b) the PtOEP/DPA/LBG ternary gel ([PtOEP] = 33 $\mu$M, [DPA] = 6.7 mM, [LBG] = 13.3 mM). Samples were dried by the extraction of DMF using supercritical $CO_2$ media. (c) Storage modulus ($G'$) and loss modulus ($G''$) versus applied shear stress on the LBG gel ([LBG] = 13.3 mM) and the PtOEP/DPA/LBG ternary gel ([PtOEP] = 33 $\mu$M, [DPA] = 6.7 mM, [LBG] = 13.3 mM) in air at room temperature. The measurement frequency was fixed as 1 Hz.

and loss moduli as a function of applied stress for the LBG gel and ternary PtOEP/DPA/LBG gel. Although the LBG gel started to flow at 14 Pa, the ternary gel was surprisingly stable up to 40 Pa. These observations clearly indicate that the gel nanofibers are significantly reinforced by the bound dye molecules.[15] The effect of dye molecules on the gel-to-sol transition temperature was further monitored by DSC measurements (Figure S3, SI). Upon increasing the concentration of DPA, the gel-to-sol phase transition temperature of LBG nanofibers showed gradual increase; $T_c$ = 43.9 °C (LBG gel), $T_c$ = 44.8 °C (LBG:DPA = 1:0.5), $T_c$ = 45.3 °C (LBG:DPA = 1:1). Thus, dye molecules are effectively integrated in the LBG nanofibers, leading to the remarkable enhancement in the rheological property and thermal stability. These observations indicate that host LBG molecules exert surprising ability to accommodate these incoming aromatic guest molecules by adaptively rearranging their hydrogen bond networks and molecular alignments.

To quantitatively understand the effect of oxygen on the TTA-UC process, we tried to obtain UC quantum yields $\Phi_{UC}$ as relative quantum yields using a standard solution, however, we found difficulty in obtaining precise $\Phi_{UC}$ values due to strong scattering of the gel samples. We thus measured absolute quantum yields of the ternary gels by using an integrating sphere and 532 nm laser as excitation source. The instrumental setup is similar to that used by Bonnet et.al. for measuring $\Phi_{UC}$ in liposomes.[16] The quantum yield is generally defined as the ratio of emitted photon numbers to absorbed photon numbers, and thus the theoretical maximum of TTA-UC efficiency is defined as 50%, by considering that the absorption of two photons is required for generating one upconverted photon.[3f,h] The experiments were conducted with incident laser power high enough to ensure the saturated TTA events and maximum $\Phi_{UC}$ values (774 mW cm$^{-2}$). We obtained $\Phi_{UC}$ of 2.7% for the deaerated PtOEP/DPA/LBG ternary gel ([PtOEP] = 33 $\mu$M, [DPA] = 6.7 mM, [LBG] = 13.3 mM), which is comparable to the reported efficient UC systems.[3h] Remarkably, this ternary gel maintained $\Phi_{UC}$ as high as 1.5% even under the air-saturated condition, confirming the excellent oxygen blocking ability of the gel system. This in-air $\Phi_{UC}$ could be further improved by increasing the acceptor concentration, providing an optimized quantum yield of ca. 3.5% for the current system (Figure S4, SI).[3f]

The oxygen blocking behavior was also confirmed by lifetime measurements of acceptor triplets. The acceptor triplet lifetime $\tau_{A,T}$ was determined as 228 and 178 $\mu$s for the deaerated and air-saturated ternary gels, respectively, by the tail-fitting of the UC emission decay curves (Figure 4).[4f,17] The ratio between

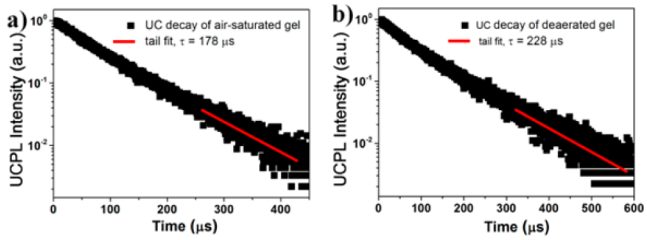


**Figure 4.** UC emission decays at 440 nm of the PtOEP/DPA/LBG ternary gel in (a) air-saturated DMF and (b) deaerated DMF under 531 nm excitation at room temperature ([PtOEP] = 33 $\mu$M, [DPA] = 6.7 mM, [LBG] = 13.3 mM). The fitting curves were obtained by considering the relationship of $I_{UC}(t) \propto \exp(-t/\tau_{UC}) = \exp(-2t/\tau_{A,T})$.[4f,17]

these two values gave a high oxygen blocking efficiency of 78%. As for the donor triplets, it is difficult to precisely assess the effect of oxygen since they undergo efficient quenching by DPA. Meanwhile, we found that 70% of PtOEP phosphorescence was quenched by DPA in the ternary gels at 77 K, where the thermal mobility of molecules was frozen and diffusion-limited quenching by oxygen became negligible (Figure S5a, SI). It is to note that both the TTET and TTA processes proceed by the electron-exchange mechanism (Dexter energy transfer), which requires orbital overlap between adjacent (<1 nm) molecules.[18] The observed efficient quenching of PtOEP by DPA therefore suggests that the most of PtOEP molecules are located adjacent to the DPA molecules. Indeed, at room temperature, the donor phosphorescence was almost quenched by the acceptor in the deaerated gel (Figure S5b, SI). All these results demonstrate that the large portion of donor and acceptor molecules are incorporated together in gel nanofibers and are protected from the oxygen quenching. It allows efficient energy migration among DPA molecules preorganized in PtOEP/DPA/LBG gels after the TTET process. The efficient inclusion of UC pairs in gel nanofibers is schematically shown in Figure 1, which gives an account of the observed surprising air-stable TTA-UC.

As all of the PtOEP, DPA, and LBG molecules are nonionic, the binding of UC pairs to nanofibers is considered to be driven by solvophobic interactions.[19] The UC pair preferred the nonpolar environment provided by the interior of gel nanofibers rather than being solvated by polar DMF. To ensure validity of the solvophobic binding, we carried out a control experiment with a nonpolar solvent $CCl_4$ that is also gelatinized by LBG. A ternary gel of PtOEP/DPA/LBG was


DOI: 10.1021/ja511061h
J. Am. Chem. Soc. 2015, 137, 1887−1894

similarly prepared in $CCl_4$ ([PtOEP] = 33 $\mu$M, [DPA] = 6.7 mM, [LBG] = 13.3 mM). In contrast to the strong UC emission shown by the air-saturated ternary DMF gel, no UC emission was observed for the ternary gel in $CCl_4$ under the same condition (Figure 5). This observation indicates that the

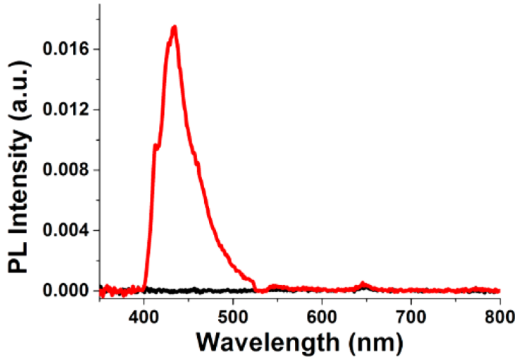


**Figure 5.** Emission spectra of the PtOEP/DPA/LBG ternary gel in air-saturated DMF (red) and $CCl_4$ (black) under identical excitation intensity at 532 nm at room temperature ([PtOEP] = 33 $\mu$M, [DPA] = 6.7 mM, [LBG] = 13.3 mM).

UC pair is dissolved in the bulk $CCl_4$ phase, where the excited triplet species are easily quenched by dissolved oxygen molecules. Although Shinkai and co-workers previously reported that organogels of metal complexes covalently modified with self-assembling units show phosphorescence even in the aerated conditions,[20] it has not been considered that organogel matrixes have the potential to protect accommodated guest molecules from oxygen quenching. The fibrous nanoassemblies of LBG serve as a superior supramolecular host to promote synergistic accumulation of TTA-UC pairs in the interior and insulate them from dissolved molecular oxygen. This is a new, surprising adaptive feature of organogels being unveiled for the first time through the integration of TTA-UC with self-assembly.

The binary PtOEP/LBG gel in DMF in the absence of the acceptor DPA showed unexpected spectral properties. The phosphorescence spectra of PtOEP in the DMF gel were measured under the deaerated and aerated conditions, respectively ([PtOEP] = 33 $\mu$M, [LBG] = 13.3 mM). It was found that the donor phosphorescence was quenched by 99% in the binary PtOEP/LBG gel in DMF under the aerated condition (Figure S6, SI). It clearly indicates that in the absence of DPA, PtOEP is not bound to LBG nanofibers. This result, however, is seemingly contradictory to the efficient TTET from PtOEP to DPA observed in the ternary PtOEP/DPA/LBG gels that showed the high UC quantum yield even under the aerobic condition. These observations are explainable only by the cooperative binding of PtOEP molecules to the DPA-enriched domains in LBG nanofibers. As described previously, the binding of DPA onto LBG nanofibers efficiently occurs in DMF, as supported by the SEM, DSC, and rheological measurements (Figure 3, and Figure S3 in SI). Under the optimized gel-forming condition for TTA-UC ([PtOEP] = 33 $\mu$M, [DPA] = 6.7 mM, [LBG] = 13.3 mM), the solvophobic binding of DPA molecules to LBG nanofibers occurs efficiently and forms aggregates in the host molecular assemblies of LBG. This is supported by the maintenance of nanofiber structures after the binding of DPA molecules (Figure 3b). It indicates the preserved hydrogen bonding networks of LBG molecules as the structural directing unit of the multicomponent fibrous nanostructures. The DPA molecules confined in the LBG nanomatrix would easily coalesce into extended aggregates, which give a $\pi$-rich nanoenvironment that shows enhanced affinity to PtOEP molecules. According to this cooperative accommodation mechanism, the donor PtOEP molecules should be well surrounded by the host of acceptor DPA molecules embedded in the nanofiber assemblies. This synergistic binding picture well describes the whole efficient TTET, triplet energy migration, and TTA processes observed for the ternary molecular systems.

After we submitted the current paper, a paper describing photon-upconversion in polymer organogels was reported by Simon and co-workers, where donor and acceptor molecules were dissolved in DMF/DMSO-based gels prepared by chemical cross-linking of poly(vinyl alcohol).[3j] They successfully observed molecular diffusion-based TTA-UC with shape-persistent gel materials, but the UC emission intensity showed a rapid decay upon continuous irradiation for about 5 min, indicative of oxygen-related photobleaching. Meanwhile, the UC emission intensity of the present PtOEP/DPA/LBG ternary gel was mostly maintained under the continuous laser excitation (Figure S7, SI). The observed difference should be related to the difference in molecular environments of the dyes; in the PtOEP/DPA/LBG ternary gel, dye molecules are accumulated inside the nanofibers where the access of oxygen molecules is intrinsically suppressed. These architectures consequently prevent the physical quenching of excited triplets and photochemical degradation of dyes, allowing the efficient energy migration among preorganized chromophores. This picture is consistent with the improved long-term stability in the ternary gel compared with solution (Figure S2, SI).

**Temperature-Triggered Modulation of TTA-UC.** Another prominent property of supramolecular gels is their thermoresponsiveness. Heating of LBG gels induce a gel-to-sol transition which is accompanied by the disassembly of fibrous gel networks, whereas the heat-dissociated components are reassembled reversibly by cooling the solution. As described previously, the ternary organogel of PtOEP/DPA/LBG showed strong UC emission by blocking the intrusion of oxygen molecules into nanofibers, whereas the TTA-UC emission was largely quenched in aerated solutions without LBG. Hence, we investigated the effect of heat-induced gel-to-sol transition with an aim to achieve temperature-triggered modulation of TTA-UC. Figure S8 in SI displays a temperature dependence of upconverted emission intensity of the ternary PtOEP/DPA/LBG system in aerated DMF ([PtOEP] = 33 $\mu$M, [DPA] = 6.7 mM, [LBG] = 13.3 mM, $\lambda_{ex}$ = 532 nm). Upon heating from 25 to 80 °C, the UC emission intensity gradually decreased and reached an almost constant value above the gel-to-sol transition temperature (~45 °C). The molecular diffusion in the higher-temperature solution phase should be high enough to complete the TTET and TTA processes, and the Dexter energy transfer is known to be temperature independent.[18,21] Also, the fluorescence quantum yield of DPA is unity independent of the solvent and temperature.[22] From this information, the decrease in UC emission intensity observed for the sol phase is ascribed to the quenching of excited triplet species by dissolved oxygen. To our interest, the UC emission intensity recovered reversibly upon cooling to 25 °C. This clearly indicates that the reassembly of ternary fibrous nanostructures occurs, which leads to simultaneous recovery of the efficient TTET and TTA-UC characteristics. The modulation of UC emission can be


DOI: 10.1021/ja511061h
J. Am. Chem. Soc. 2015, 137, 1887−1894

repeated reversibly, as shown in Figure 6. When the sample was heated for a long-time (>2 h) at 90 °C, the UC emission intensity was further decreased, indicating slow diffusion of molecular oxygen in the hot solution.

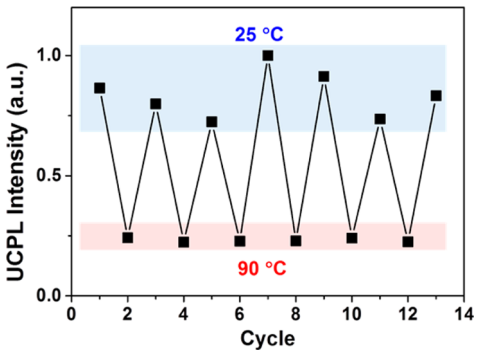


**Figure 6.** UC emission intensity of the PtOEP/DPA/LBG ternary gel in air-saturated DMF at 435 nm in the heating–cooling cycles ([PtOEP] = 33 $\mu$M, [DPA] = 6.7 mM, [LBG] = 13.3 mM; $\lambda_{ex}$ = 532 nm).

**Low UC Threshold Excitation Intensity $I_{th}$ in the Ternary Gels.** It is crucial that high TTA-UC efficiency is attainable with reasonably weak excitation light such as sunlight. A useful figure-of-merit of TTA-UC is given by a threshold excitation intensity $I_{th}$, above which the upconversion efficiency $\Phi_{UC}$ is maximized.[17] When the sunlight is used as an excitation source, $I_{th}$ should therefore be lower than the solar irradiance (the integration of AM 1.5 solar spectrum from 527 to 537 nm gives 1.6 mW cm$^{-2}$). In deaerated solutions, the molecular diffusion is usually high enough to obtain $I_{th}$ values which are lower than the solar irradiance.[3f] Meanwhile, under air-saturated conditions, TTA-UC is hampered by the massive quenching of excited triplet states by dissolved oxygen. To avoid the quenching by oxygen, specific polymers or viscous liquids has been employed as matrixes to slow down the diffusion of oxygen. However, in these matrixes, the $I_{th}$ values remained high; $I_{th}$ values of ca. 100, 20, and 4.3 mW cm$^{-2}$ were reported for polyurethane[4g,h] and poly(butylacrylate)[23] matrixes. Kim and co-workers reported $I_{th}$ of ∼200 mW cm$^{-2}$ in a mixture of hexadecane and polyisobutylene,[3e] whereas Li et.al. obtained $I_{th}$ of ∼60 mW cm$^{-2}$ in BSA–dextran-stabilized soybean oil.[3g] In the conventional air-stable TTA-UC systems, TTET and TTA processes occur based on the molecular diffusion and collision, where the diffusion of molecules in these matrixes is inevitably low. In remarkable contrast to the previous air-resistant systems, the present supramolecular gels showed low-power TTA-UC, which indicates the contribution of efficient triplet energy transfer and migration in nanofibers, as discussed below.

In general, the upconverted emission intensity through sensitized TTA shows a quadratic dependence to the incident light power in the weak excitation region as expected for the bimolecular annihilation process. In this regime, TTA is inefficient because of the prevailing nonradiative decay of acceptor triplets. Meanwhile, by increasing the incident power to $I_{th}$, TTA provides the main deactivation channel for the acceptor triplet. Consequently, at the incident light power density of $I_{th}$, the incident power dependence changes from quadratic to linear and above that the upconversion efficiency $\Phi_{UC}$ is maximized. Figure 7 presents a double logarithm plot

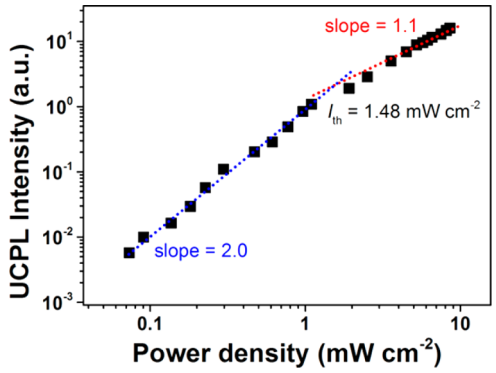


**Figure 7.** TTA-UC emission intensity observed for PtOEP/DPA/LBG ternary gel as a function of the 532 nm excitation power density in air-saturated DMF at room temperature ([PtOEP] = 33 $\mu$M, [DPA] = 6.7 mM, and [LBG] = 13.3 mM). The dashed lines are fitting results with slopes of 2.0 (blue) and 1.1 (red), and $I_{th}$ was determined as 1.48 mW cm$^{-2}$ from the crossing point of these two lines.

for the UC emission intensity of the air-saturated PtOEP/DPA/LBG ternary gel as a function of incident light power density. At the lower-power regime (<1.48 mW cm$^{-2}$), a slope close to 2 was observed, whereas it changed to ca. 1 at a higher power density (>1.48 mW cm$^{-2}$). The observed quadratic dependence of UC emission intensity at lower incident power density provides decisive evidence for TTA-based UC in the ternary gel. Note that the sample remained intact during the excitation power dependence measurements. The UC emission intensity was measured by changing the excitation power from low to high power density, and then continuously from high to low power density at the same sample spot (Figure S9, SI). The UC emission intensity showed a good reversibility, indicating that the sample decomposition did not take place. Remarkably, the observed $I_{th}$ of 1.48 mW cm$^{-2}$ under the air-saturated condition is lower than the solar irradiance of 1.6 mW cm$^{-2}$ at 532 ± 5 nm, indicating excellent performance of the present supramolecular TTA-UC system.

To scrutinize the observed remarkably low $I_{th}$ value, we estimated the diffusion constant $D_T$ of acceptor triplet in the deaerated PtOEP/DPA/LBG ternary gel ([PtOEP] = 33 $\mu$M, [DPA] = 6.7 mM, [LBG] = 13.3 mM) by using the following equation,[17,21] where $a_0$ is the effective triplet–triplet interaction distance (9.1 Å for DPA triplet), $\alpha$ is the absorption coefficient at excitation wavelength 532 nm (4.19 cm$^{-1}$), and $\Phi_{ET}$ is the donor-to-acceptor TTET efficiency.

$$I_{th} = (8\pi D_T a_0 \alpha \Phi_{ET})^{-1} \tau_{A,T}^{-2} \quad (1)$$

The $I_{th}$ value for deaerated ternary gel was determined as 0.75 mW cm$^{-2}$ that was a little lower than that observed for the air-saturated gel, reflecting the elimination of oxygen quenching process as observed in Figure 4. A high $\Phi_{ET}$ value of 97.7% was obtained by the ratio between the donor phosphorescence intensity with and without the acceptor in the deaerated gel (Figure S5b, SI). Accordingly, $D_T$ of 6.5 × 10$^{-4}$ cm$^2$ s$^{-1}$ is obtained for the PtOEP/DPA/LBG ternary gel. Very interestingly, this $D_T$ value is 1 order of magnitude larger than the diffusion constant of DPA in the low-viscosity solvents (1.2 × 10$^{-5}$ cm$^2$ s$^{-1}$).[21] This is surprising because the dynamic molecular diffusion in rigid crystal-like gel fibers should be much suppressed compared to the previous low-viscosity solvent systems. The large $D_T$ value then must indicate fast triplet energy migration among the densely organized dyes in


DOI: 10.1021/ja511061h
J. Am. Chem. Soc. 2015, 137, 1887–1894

the gel nanofibers, which provides a reasonable account for the observed low $I_{th}$ value. The contribution of triplet energy migration for UC was then confirmed by low-temperature measurements at 77 K, where the molecular diffusion is frozen. UC emission was clearly observed even at 77K, with a high donor-to-acceptor TTET efficiency $\Phi_{ET}$ of 70% (Figures S5a and S10, SI). This clearly indicates the proximity of donor to acceptor in the nanofiber interior, supporting the cooperative accumulation of these dyes in nanofibers. On the basis of these low-temperature experiments, we conclude that the triplet energy transfer and migration do occur even in the frozen nanofiber matrixes.

These observations clearly unveiled the unique features of TTA-UC systems in organogel matrixes; even in the matrixes of crystal-like order, efficient UC is achieved at low excitation power by virtue of the efficient triplet energy transfer and migration. In our system, PtOEP is effectively adsorbed to the binary DPA/LBG nanofibers, exerting surprisingly efficient TTA-UC even at remarkably low incident light density (i.e., low $I_{th}$ value). The synergistic integration of donor–acceptor pairs is reminiscent of the biological photon-harvesting apparatuses in which excitation light energy is effectively harvested and converted in the array of photosynthetic pigments embedded in biomembranes.[2]

**Universality of In-Air TTA-UC in Cogels.** To generalize the concept of nanomatrix-assisted TTA-UC, three additional different UC pairs were introduced in the nanofiber of LBG gels in DMF: $PdPc(OBu)_8$/rubrene for NIR-to-visible UC,[24] PtTPBP/BPEA for red-to-cyan UC,[25] and $Ir(C6)_2(acac)$/DBP for visible-to-UV UC.[26] In air-saturated DMF solutions, all of the three UC pairs showed no UC emission in the absence of LBG (excitation power density was around 100 mW $cm^{-2}$). However, when they are introduced in LBG gels in DMF, all the ternary gels exhibited strong UC emissions even under air-saturated conditions (Figure 8). The light conversions from NIR (730 nm) to yellow (570 nm), from red (635 nm) to cyan (507 nm), and from blue (445 nm) to UV (377 nm) were confirmed by the photoluminescence spectra (Figure S11, SI). The TTA-based UC mechanism of these UC systems was confirmed by the transitions of UC emission intensity from quadratic to linear dependence on excitation power density (Figure S11, SI), which showed relatively low $I_{th}$ values.

Similarly to the case of ternary PtOEP/DPA/LBG gels, no UC emission was observed for the ternary gels when nonpolar $CCl_4$ was used as a solvent. Thus, all the donors and acceptors show solvophobic accumulation into gel networks when polar DMF was employed as solvent, which enabled effective shielding of the TTA-UC processes against dissolved oxygen molecules. It is remarkable that the present supramolecular nanomatrix approach offers the general methodology of efficient TTA-UC workable in air.

## ■ CONCLUSIONS

Inspired by the sophisticated energy harvesting systems in photosynthetic biomembranes, we developed a simple yet universal approach for developing TTA-based UC gels by the adaptive and cooperative accumulation of various donor–acceptor UC pairs in supramolecular nanofibers. Despite the considerable effort expended on the study of singlet energy transfer and migration characteristics in dense dye assemblies,[1] the development of triplet energy transfer and TTA-UC events in supramolecular nanomatrixes remained unexplored. The present self-assembly system offers unprecedented opportunities for the efficient triplet energy transfer, migration, and consequent TTA-UC phenomena even under aerated conditions. Note that the in-air stability and low threshold excitation intensity $I_{th}$ have been incompatible in the past TTA-UC systems. The use of gel nanofibers as adaptive nanomatrixes allows confinement and condensation of photofunctional elements in nanospace, by virtue of solvophobic interactions in organic media. The developed hydrogen bond networks formed by the aligned LBG molecules would be contributing to the screening of molecular oxygen to the solvophobic interior of nanofibers, as a similar oxygen blocking property has also been observed for aqueous nanoparticles of coordination networks.[27] The integration of TTA-UC with self-assembly thus resolves the long-term issue in TTA-UC and renovates the field by introducing the triplet energy migration process. The concept of light-harvesting, adaptive nanofiber gel networks with unprecedented oxygen barrier properties would be widely applicable to design functional molecular systems in many disciplines.

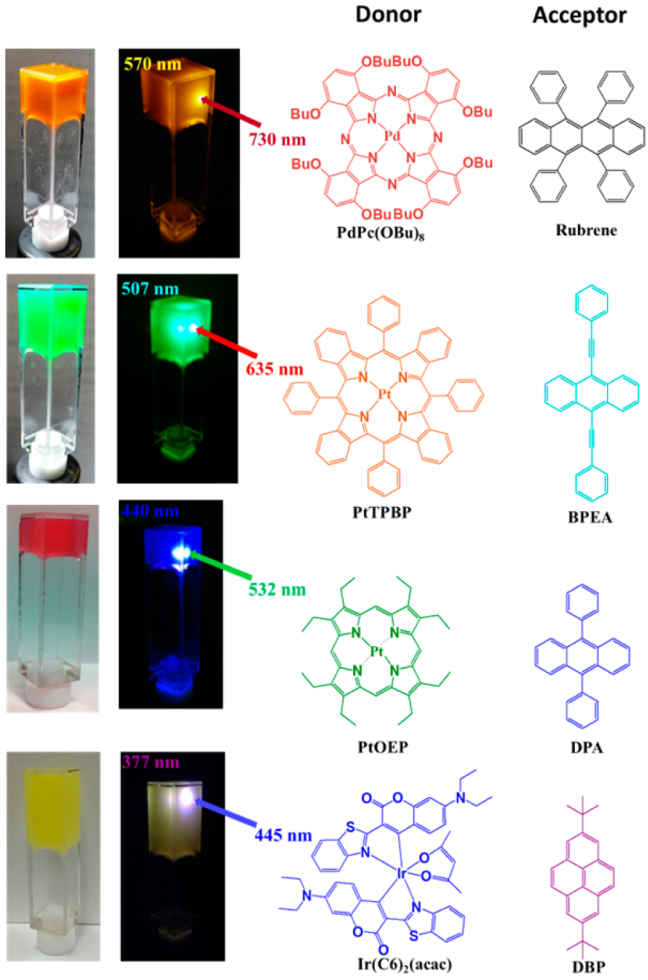


**Figure 8.** Photographs of the UC cogels in air-saturated DMF. Typical UC pairs were used to form ternary gels: $PdPc(OBu)_8$/rubrene/LBG gel for NIR-to-visible UC ([$PdPc(OBu)_8$] = 67 $\mu$M, [rubrene] = 6.7 mM, [LBG] = 13.3 mM), PtTPBP/BPEA/LBG gel for red-to-cyan UC ([PtTPBP] = 67 $\mu$M, [BPEA] = 6.7 mM, [LBG] = 13.3 mM), PtOEP/DPA/LBG gel for green-to-blue UC ([PtOEP] = 33 $\mu$M, [DPA] = 6.7 mM [LBG] = 13.3 mM), and $Ir(C6)_2(acac)$/DBP/LBG gel for blue-to-UV UC ([$Ir(C6)_2(acac)$] = 67 $\mu$M, [DBP] = 6.7 mM, [LBG] = 13.3 mM). Short pass filters were used to remove the scattered excitation lights.


DOI: 10.1021/ja511061h
J. Am. Chem. Soc. 2015, 137, 1887–1894

## ■ ASSOCIATED CONTENT

### Supporting Information

Time-dependent UC emission intensity, DSC, phosphorescence spectra, temperature-dependent UC emission intensity, and detailed characterizations of NIR-to-yellow, red-to-cyan, and blue-to-UV upconverting cogels. This material is available free of charge via the Internet at http://pubs.acs.org.

## ■ AUTHOR INFORMATION


### Corresponding Authors

*yanai@mail.cstm.kyushu-u.ac.jp
*n-kimi@mail.cstm.kyushu-u.ac.jp


### Notes

The authors declare no competing financial interest.

## ■ ACKNOWLEDGMENTS

This work was supported by a Grants-in-Aid for Scientific Research (S) (25220805), a Grants-in-Aid for Young Scientists (B) (26810036), a Grant-in-Aid for Scientific Research on Innovative Area (26104529) from the Ministry of Education, Culture Sports, Science and Technology of Japan, and a research grant from The Noguchi Institute.

## ■ REFERENCES


(1) (a) Dekker, J. P.; Boekema, E. J. *Biochim. Biophys. Acta, Bioenerg.* **2005**, *1706*, 12. (b) Strümpfer, J.; Şener, M.; Schulten, K. *J. Phys. Chem. Lett.* **2012**, *3*, 536.

(2) (a) Nakashima, T.; Kimizuka, N. *Adv. Mater.* **2002**, *14*, 1113. (b) Calzaferri, G.; Huber, S.; Maas, H.; Minkowski, C. *Angew. Chem., Int. Ed.* **2003**, *42*, 3732. (c) Choi, M. S.; Yamazaki, T.; Yamazaki, I.; Aida, T. *Angew. Chem., Int. Ed.* **2004**, *43*, 150. (d) Ajayaghosh, A.; Praveen, V. K.; Vijayakumar, C. *Chem. Soc. Rev.* **2008**, *37*, 109.

(3) (a) Baluschev, S.; Miteva, T.; Yakutkin, V.; Nelles, G.; Yasuda, A.; Wegner, G. *Phys. Rev. Lett.* **2006**, *97*, 143903. (b) Cheng, Y. Y.; Khoury, T.; Clady, R.; Tayebjee, M. J. Y.; Ekins-Daukes, N. J.; Crossley, M. J.; Schmidt, T. W. *Phys. Chem. Chem. Phys.* **2010**, *12*, 66. (c) Singh-Rachford, T. N.; Castellano, F. N. *Coord. Chem. Rev.* **2010**, *254*, 2560. (d) Zhao, J. Z.; Ji, S. M.; Guo, H. M. *RSC Adv.* **2011**, *1*, 937. (e) Kim, J. H.; Kim, J. H. *J. Am. Chem. Soc.* **2012**, *134*, 17478. (f) Monguzzi, A.; Tubino, R.; Hoseinkhani, S.; Campione, M.; Meinardi, F. *Phys. Chem. Chem. Phys.* **2012**, *14*, 4322. (g) Liu, Q.; Yin, B. R.; Yang, T. S.; Yang, Y. C.; Shen, Z.; Yao, P.; Li, F. Y. *J. Am. Chem. Soc.* **2013**, *135*, 5029. (h) Gray, V.; Dzebo, D.; Abrahamsson, M.; Albinsson, B.; Moth-Poulsen, K. *Phys. Chem. Chem. Phys.* **2014**, *16*, 10345. (i) Monguzzi, A.; Braga, D.; Gandini, M.; Holmberg, V. C.; Kim, D. K.; Sahu, A.; Norris, D. J.; Meinardi, F. *Nano Lett.* **2014**, *14*, 6644. (j) Vadrucci, R.; Weder, C.; Simon, Y. C. *Mater. Horiz.* **2015**, *2*, 120.

(4) (a) Laquai, F.; Wegner, G.; Im, C.; Busing, A.; Heun, S. *J. Chem. Phys.* **2005**, *123*, 074902. (b) Singh-Rachford, T. N.; Lott, J.; Weder, C.; Castellano, F. N. *J. Am. Chem. Soc.* **2009**, *131*, 12007. (c) Monguzzi, A.; Tubino, R.; Meinardi, F. *J. Phys. Chem. A* **2009**, *113*, 1171. (d) Tanaka, K.; Inafuku, K.; Chujo, Y. *Chem. Commun.* **2010**, *46*, 4378. (e) Simon, Y. C.; Weder, C. *J. Mater. Chem.* **2012**, *22*, 20817. (f) Monguzzi, A.; Frigoli, M.; Larpent, C.; Tubino, R.; Meinardi, F. *Adv. Funct. Mater.* **2012**, *22*, 139. (g) Kim, J. H.; Deng, F.; Castellano, F. N.; Kim, J. H. *Chem. Mater.* **2012**, *24*, 2250. (h) Jiang, Z.; Xu, M.; Li, F. Y.; Yu, Y. L. *J. Am. Chem. Soc.* **2013**, *135*, 16446. (i) Duan, P. F.; Yanai, N.; Kimizuka, N. *J. Am. Chem. Soc.* **2013**, *135*, 19056. (j) Svagan, A. J.; Busko, D.; Avlasevich, Y.; Glasser, G.; Baluschev, S.; Landfester, K. *ACS Nano* **2014**, *8*, 8198. (k) Marsico, F.; Turshatov, A.; Pekoz, R.; Avlasevich, Y.; Wagner, M.; Weber, K.; Donadio, D.; Landfester, K.; Baluschev, S.; Wurm, F. R. *J. Am. Chem. Soc.* **2014**, *136*, 11057.

(5) (a) Terech, P.; Weiss, R. G. *Chem. Rev.* **1997**, *97*, 3133. (b) Kimizuka, N.; Shimizu, M.; Fujikawa, S.; Fujimura, K.; Sano, M.; Kunitake, T. *Chem. Lett.* **1998**, 967. (c) Liu, X. Y. In *Low Molecular Mass Gelators: Design, Self-Assembly, Function*; Fages, F., Ed., Springer: New York, 2005; Vol. 256. (d) Sangeetha, N. M.; Maitra, U. *Chem. Soc. Rev.* **2005**, *34*, 821. (e) Nakashima, T.; Kimizuka, N. *Polym. J.* **2012**, *44*, 665.

(6) Dawn, A.; Shiraki, T.; Haraguchi, S.; Tamaru, S.; Shinkai, S. *Chem.—Asian J.* **2011**, *6*, 266.

(7) (a) Lal, M.; Pakatchi, S.; He, G. S.; Kim, K. S.; Prasad, P. N. *Chem. Mater.* **1999**, *11*, 3012. (b) Duan, P. F.; Li, Y. G.; Jiang, J.; Wang, T. Y.; Liu, M. H. *Sci. China Chem.* **2011**, *54*, 1051.

(8) (a) Lamansky, S.; Djurovich, P.; Murphy, D.; Abdel-Razzaq, F.; Lee, H. E.; Adachi, C.; Burrows, P. E.; Forrest, S. R.; Thompson, M. E. *J. Am. Chem. Soc.* **2001**, *123*, 4304. (b) Borisov, S. M.; Klimant, I. *Anal. Chem.* **2007**, *79*, 7501.

(9) Li, Y. G.; Wang, T. Y.; Liu, M. H. *Soft Matter* **2007**, *3*, 1312.

(10) Moneghini, M.; Kikic, I.; Voinovich, D.; Perissutti, B.; Filipovic-Grcic, J. *Int. J. Pharm.* **2001**, *222*, 129.

(11) (a) Melhuish, W. H. *J. Phys. Chem.* **1961**, *65*, 229. (b) Suzuki, K.; Kobayashi, A.; Kaneko, S.; Takehira, K.; Yoshihara, T.; Ishida, H.; Shiina, Y.; Oishic, S.; Tobita, S. *Phys. Chem. Chem. Phys.* **2009**, *11*, 9850.

(12) Lakowicz, J. R. *Principles of fluorescence spectroscopy*, 3rd ed.; Kluwer Academic/Plenum Publishers: New York, 2006.

(13) (a) Duan, P. F.; Li, Y. G.; Liu, M. H. *Sci. China Chem.* **2010**, *53*, 432. (b) Lv, K.; Qin, L.; Wang, X. F.; Zhang, L.; Liu, M. H. *Phys. Chem. Chem. Phys.* **2013**, *15*, 20197.

(14) (a) Takehara, M. *Colloids Surf.* **1989**, *38*, 149. (b) Kira, Y.; Okazaki, Y.; Sawada, T.; Takafuji, M.; Ihara, H. *Amino Acids* **2010**, *39*, 587.

(15) Tian, Y.; Zhang, L.; Duan, P. F.; Liu, F. Y.; Zhang, B. Q.; Liu, C. Y.; Liu, M. H. *New J. Chem.* **2010**, *34*, 2847.

(16) Askes, S. H. C.; Bahreman, A.; Bonnet, S. *Angew. Chem., Int. Ed.* **2014**, *53*, 1029.

(17) Monguzzi, A.; Mezyk, J.; Scotognella, F.; Tubino, R.; Meinardi, F. *Phys. Rev. B* **2008**, *78*, 195112.

(18) Turro, N. J.; Ramamurthy, V.; Scaiano, J. C. *Modern Molecular Photochemistry of Organic Molecules*; University Science Books: Sausalito, CA, 2010.

(19) Kunitake, T. *Angew. Chem., Int. Ed.* **1992**, *31*, 709.

(20) (a) Shirakawa, M.; Fujita, N.; Tani, T.; Kaneko, K.; Shinkai, S. *Chem. Commun.* **2005**, 4149. (b) Shirakawa, M.; Fujita, N.; Tani, T.; Kaneko, K.; Ojima, M.; Fujii, A.; Ozaki, M.; Shinkai, S. *Chem.—Eur. J.* **2007**, *13*, 4155.

(21) Monguzzi, A.; Tubino, R.; Meinardi, F. *Phys. Rev. B* **2008**, *77*, 155122.

(22) Ting, C. H. *Chem. Phys. Lett.* **1967**, *1*, 335.

(23) Monguzzi, A.; Bianchi, F.; Bianchi, A.; Mauri, M.; Simonutti, R.; Ruffo, R.; Tubino, R.; Meinardi, F. *Adv. Energy Mater.* **2013**, *3*, 680.

(24) Singh-Rachford, T. N.; Castellano, F. N. *J. Phys. Chem. A* **2008**, *112*, 3550.

(25) Baluschev, S.; Yakutkin, V.; Miteva, T.; Wegner, G.; Roberts, T.; Nelles, G.; Yasuda, A.; Chernov, S.; Aleshchenkov, S.; Cheprakov, A. *New J. Phys.* **2008**, *10*, 013007.

(26) (a) Zhao, W.; Castellano, F. N. *J. Phys. Chem. A* **2006**, *110*, 11440. (b) Duan, P. F.; Yanai, N.; Kimizuka, N. *Chem. Commun.* **2014**, *50*, 13111.

(27) Nishiyabu, R.; Aime, C.; Gondo, R.; Noguchi, T.; Kimizuka, N. *Angew. Chem., Int. Ed.* **2009**, *48*, 9465.




DOI: 10.1021/ja511061h
*J. Am. Chem. Soc.* 2015, 137, 1887−1894